J|A|C|S ARTICLES

Published on Web 12/03/2010

Experimental and Computational Investigation of C−N Bond Activation in Ruthenium N-Heterocyclic Carbene Complexes

L. Jonas L. Häller,[†] Michael J. Page,[‡] Stefan Erhardt,[†,§] Stuart A. Macgregor,*[,†] Mary F. Mahon,[‡] M. Abu Naser,[†] Andrea Vélez,[†] and Michael K. Whittlesey*[,‡]

School of Engineering and Physical Sciences, Heriot-Watt University, Edinburgh EH14 4AS, and Department of Chemistry, University of Bath, Claverton Down, Bath BA2 7AY, United Kingdom

Received October 28, 2010; E-mail: S.A.Macgregor@hw.ac.uk; chsmkw@bath.ac.uk

Abstract: A combination of experimental studies and density functional theory calculations is used to study C−N bond activation in a series of ruthenium *N*-alkyl-substituted heterocyclic carbene (NHC) complexes. These show that prior C−H activation of the NHC ligand renders the system susceptible to irreversible C−N activation. In the presence of a source of HCl, C−H activated Ru(I^{i}Pr$_2$Me$_2$)′(PPh$_3$)$_2$(CO)H (**1**, I^{i}Pr$_2$Me$_2$ = 1,3-diisopropyl-4,5-dimethylimidazol-2-ylidene) reacts to give Ru(I^{i}PrHMe$_2$)(PPh$_3$)$_2$(CO)HCl (**2**, I^{i}PrHMe$_2$ = 1-isopropyl-4,5-dimethylimidazol-2-ylidene) and propene. The mechanism involves (i) isomerization to a *trans*-phosphine isomer, **1c**, in which hydride is trans to the metalated alkyl arm, (ii) C−N cleavage to give an intermediate propene complex with a C2-metalated imidazole ligand, and (iii) N-protonation and propene/Cl$^-$ substitution to give **2**. The overall computed activation barrier ($\Delta E^{\ddagger}_{calcd}$) corresponds to the isomerization/C−N cleavage process and has a value of +24.4 kcal/mol. C−N activation in **1c** is promoted by the relief of electronic strain arising from the trans disposition of the high-trans-influence hydride and alkyl ligands. Experimental studies on analogues of **1** with different C4/C5 carbene backbone substituents (Ru(I^{i}Pr$_2$Ph$_2$)′(PPh$_3$)$_2$(CO)H, Ru(I^{i}Pr$_2$)′(PPh$_3$)$_2$(CO)H) or different N-substituents (Ru(IEt$_2$Me$_2$)′(PPh$_3$)$_2$(CO)H) reveal that Ph substituents promote C−N activation. Calculations confirm that Ru(I^{i}Pr$_2$Ph$_2$)′(PPh$_3$)$_2$(CO)H undergoes isomerization/C−N bond cleavage with a low barrier of only +21.4 kcal/mol. Larger *N*-alkyl groups also facilitate C−N bond activation (Ru(I^{t}Bu$_2$Me$_2$)′(PPh$_3$)$_2$(CO)H, $\Delta E^{\ddagger}_{calcd}$ = +21.3 kcal/mol), and in this case the reaction is promoted by the formation of the more highly substituted 2-methylpropene.

Introduction

N-heterocyclic carbenes (NHCs) are now universally recognized as being a class of ligands that can impart exceptional catalytic activity onto metal centers. Numerous reviews and, more recently, a number of textbooks have detailed the role of NHCs in enhancing the ability of metals to catalyze a range of reactions, most commonly metathesis, C−C coupling, and H−X addition across C═O and C═C bonds.[1] Consideration of the metathesis literature highlights another, less appreciated and certainly less well understood aspect of M−NHC complexes, that is, their susceptibility to undergo degradation via bond activation reactions.[2] Thus, Grubbs, Piers, and Dorta have all shown during efforts to prepare more active ruthenium-based metathesis catalysts the occurrence of irreversible C−H activation of an N-substituent on the carbene, resulting in the catalyst lifetime being compromised and the catalyst efficiency being reduced.[3]

Ruthenium complexes appear to be particularly prone to M−NHC degradation reactions, with not only C−H activation, but also C−C activation and migration/insertion reactions being documented.[4] In 2006, we showed that treatment of Ru(PPh$_3$)$_3$(CO)HCl with 2 equiv of 1,3-diisopropyl-4,5-dimethylimidazol-2-ylidene (I^{i}Pr$_2$Me$_2$) at 70 °C afforded a mixture of products consisting not only of the C−H activated carbene complex *cis*-Ru(I^{i}Pr$_2$Me$_2$)′(PPh$_3$)$_2$(CO)H (**1a**), but also more unexpectedly, of **2** (Scheme 1), which results from C−N activation of one of the N−^{i}Pr linkages in the carbene.[5] Upon

[†] Heriot-Watt University.
[‡] University of Bath.
[§] Present address: Departamento de Química, Faculdade de Ciências e Tecnologia, Universidade Nova de Lisboa, 2829-516 Caparica, Portugal.

(1) (a) Bourissou, D.; Guerret, O.; Gabbaï, F. P.; Bertrand, G. *Chem. Rev.* **2000**, *100*, 39. (b) Herrmann, W. A.; Weskamp, T.; Böhm, V. P. W. *Adv. Organomet. Chem.* **2001**, *48*, 1. (c) Herrmann, W. A. *Angew. Chem., Int. Ed.* **2002**, *41*, 1290. (d) *N-Heterocyclic Carbenes in Synthesis*; Nolan, S. P., Ed.; Wiley-VCH: Weinheim, Germany, 2006. (e) *N-Heterocyclic Carbenes in Transition Metal Catalysis*; Glorius, F., Ed.; Springer-Verlag: Heidelberg, Germany, 2007. (f) Kantchev, E. A. B.; O' Brien, C. J.; Organ, M. G. *Angew. Chem., Int. Ed.* **2007**, *46*, 2768. (g) Hahn, F. E.; Jahnke, M. C. *Angew. Chem., Int. Ed.* **2008**, *47*, 3122. (h) Marion, N.; Nolan, S. P. *Acc. Chem. Res.* **2008**, *41*, 1440. (i) Díez-González, S.; Marion, N.; Nolan, S. P. *Chem. Rev.* **2009**, *109*, 3612. (j) Poyatos, M.; Mata, J. A.; Peris, E. *Chem. Rev.* **2009**, *109*, 3677. (k) Dröge, T.; Glorius, F. *Angew. Chem., Int. Ed.* **2010**, *49*, 6940. (k) *N-Heterocyclic Carbenes in Transition Metal Catalysis and Organocatalysis*; Cazin, C. S. J., Ed.; Springer-Verlag: Heidelberg, Germany, 2011.

(2) (a) Crudden, C. M.; Allen, D. P. *Coord. Chem. Rev.* **2004**, *248*, 2247. (b) Cavell, K. J. *Dalton Trans.* **2008**, 6676. (c) Albrecht, M. *Chem. Rev.* **2010**, *110*, 576.

(3) (a) Trnka, T. M.; Morgan, J. P.; Sanford, M. S.; Wilhelm, T. E.; Scholl, M.; Choi, T.-L.; Ding, S.; Day, M. W.; Grubbs, R. H. *J. Am. Chem. Soc.* **2003**, *125*, 2546. (b) Hong, S. H.; Wenzel, A. G.; Salguero, T. T.; Day, M. W.; Grubbs, R. H. *J. Am. Chem. Soc.* **2007**, *129*, 7961. (c) Leitao, E. M.; Dubberley, S. R.; Piers, W. E.; Wu, Q.; McDonald, R. *Chem.—Eur. J.* **2008**, *14*, 11565. (d) Vieille-Petit, L.; Luan, X.; Gatti, M.; Blumentritt, S.; Linden, A.; Clavier, H.; Nolan, S. P.; Dorta, R. *Chem. Commun.* **2009**, 3783.

 10.1021/ja109702h © **2010 American Chemical Society**

Scheme 1

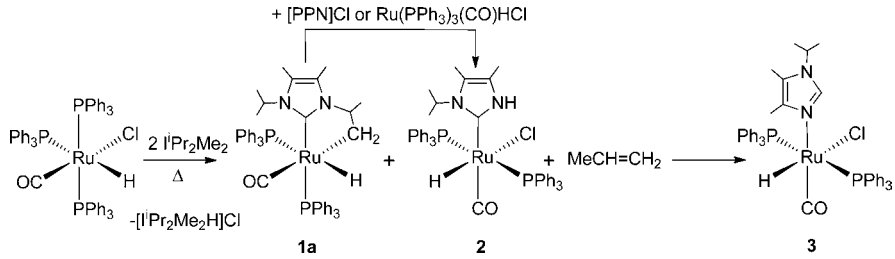

further heating, **2** underwent tautomerism to the N-bound species **3** in the presence of excess NHC.[6,7]

C−N activation of NHCs was first described only in 2004 by Cloke, Caddick, and co-workers.[8] Exposure of a THF solution of $Ni(cod)_2$ and excess 1,3-di-*tert*-butylimidazol-2-ylidene (I^tBu) to sunlight for two weeks yielded a dinuclear Ni(II) species containing two C−N activated I^tBu ligands. Shorter irradiation times led to the isolation of an intermediate species containing a C−H activated *N*-^{t}Bu group, which upon heating with additional I^tBu at 70 °C afforded the same final C−N activated product, along with isobutene. The importance of C−H activation as a forerunner to C−N activation suggested by the nickel work was reinforced by our observations on ruthenium that (i) direct heating of the C−H activated complex **1a** in the presence of a chloride source (either bis(triphenylphosphoranylidene)ammonium chloride ([PPN]Cl) or $Ru(PPh_3)_3(CO)HCl$) gave a mixture of **2** and **3** and (ii) C−N activation was completely shut down when $Ru(PPh_3)_3(CO)HCl$ was reacted with $I^iPr_2Me_2$ under 1 atm of H_2, conditions under which C−H activation is reversible.

C−N activation has now been observed in a number of both early (Y, Zr) and late (Rh, Ir, Pd) metal NHC complexes.[9] However, these reactions either involve poorly defined metal complexes generated in situ using imidazolium salt precursors or take place under highly forcing or heterogeneous conditions. Such processes do not lend themselves to detailed mechanistic studies or the thorough characterization of decomposition products that is so essential (as highlighted by Grubbs[3b]) if a proper understanding of decomposition pathways is to be obtained. In contrast, our ruthenium system provides a well-defined set of complexes that allow for the first time an understanding of the C−N activation decomposition reaction. Herein, we report a combined experimental and computational mechanistic study of C−N bond activation originating in **1a** that provides insight into (i) how C−N activation takes place, (ii) the role of C−H activation, and (iii) the importance of N- and backbone NHC-substituents and metal ancillary ligands. Of particular note is the finding that C−N activation is intimately linked to the presence of a hydride ligand, highlighting the fact that NHC complexes susceptible to C−H activation may be particularly vulnerable to a subsequent irreversible decomposition via C−N activation.

Results and Discussion

Further Experimental Observations on C−N Activation. The transformation of **1a** to **2** involves a number of separate processes, including not only cleavage of the C−N bond but also reorientation from a *cis*- to a *trans*-phosphine arrangement, loss of propene, and, ultimately, addition of "HCl". As shown in Scheme 1, reaction from $Ru(PPh_3)_3(CO)HCl$ requires at least 2 equiv of $I^iPr_2Me_2$, suggesting that the HCl lost upon converting $Ru(PPh_3)_3(CO)HCl$ to **1a** is trapped as the imidazolium chloride

(4) (a) Jazzar, R. F. R.; Macgregor, S. A.; Mahon, M. F.; Richards, S. P.; Whittlesey, M. K. *J. Am. Chem. Soc.* **2002**, *124*, 4944. (b) Giunta, D.; Hölscher, M.; Lehmann, C. W.; Mynott, R.; Wirtz, C.; Leitner, W. *Adv. Synth. Catal.* **2003**, *345*, 1139. (c) Burling, S.; Mahon, M. F.; Paine, B. M.; Whittlesey, M. K.; Williams, J. M. J. *Organometallics* **2004**, *23*, 4537. (d) Abdur-Rashid, K.; Fedorkiw, T.; Lough, A. J.; Morris, R. H. *Organometallics* **2004**, *23*, 86. (e) Cabeza, J. A.; del Río, I.; Miguel, D.; Sánchez-Vega, M. G. *Chem. Commun.* **2005**, 3956. (f) Galan, B. R.; Gembicky, M.; Dominiak, P. M.; Keister, J. B.; Diver, S. T. *J. Am. Chem. Soc.* **2005**, *127*, 15702. (g) Becker, E.; Stingl, V.; Dazinger, G.; Puchberger, M.; Mereiter, K.; Kirchner, K. *J. Am. Chem. Soc.* **2006**, *128*, 6572. (h) Hong, S. H.; Chlenov, A.; Day, M. W.; Grubbs, R. H. *Angew. Chem., Int. Ed.* **2007**, *46*, 5148. (i) Burling, S.; Paine, B. M.; Nama, D.; Brown, V. S.; Mahon, M. F.; Prior, T. J.; Pregosin, P. S.; Whittlesey, M. K.; Williams, J. M. J. *J. Am. Chem. Soc.* **2007**, *129*, 1987. (j) Galan, B. R.; Pitak, M.; Gembicky, M.; Keister, J. B.; Diver, S. T. *J. Am. Chem. Soc.* **2009**, *131*, 6822. (k) Burling, S.; Mas-Marzá, E.; Valpuesta, J. E. V.; Mahon, M. F.; Whittlesey, M. K. *Organometallics* **2009**, *28*, 6676. (l) Benhamou, L.; Wolf, J.; César, V.; Labande, A.; Poli, R.; Lugan, N.; Lavigne, G. *Organometallics* **2009**, *28*, 6981. (m) Armstrong, R.; Ecott, C.; Mas-Marzá, E.; Page, M. J.; Mahon, M. F.; Whittlesey, M. K. *Organometallics* **2010**, *29*, 991.

(5) Burling, S.; Mahon, M. F.; Powell, R. E.; Whittlesey, M. K.; Williams, J. M. J. *J. Am. Chem. Soc.* **2006**, *128*, 13702.

(6) For other tautomerization processes, see: (a) Sundberg, R. J.; Bryan, R. F.; Taylor, I. F.; Taube, H. *J. Am. Chem. Soc.* **1974**, *96*, 381. (b) Sini, G.; Eisenstein, O.; Crabtree, R. H. *Inorg. Chem.* **2002**, *41*, 602. (c) Wiedemann, S. H.; Lewis, J. C.; Ellman, J. A.; Bergman, R. G. *J. Am. Chem. Soc.* **2006**, *128*, 2452. (d) Alvarez, E.; Conejero, S.; Paneque, M.; Petronilho, A.; Poveda, M. L.; Serrano, O.; Carmona, E. *J. Am. Chem. Soc.* **2006**, *128*, 13060. (e) Alvarez, E.; Conejero, S.; Lara, P.; López, J. A.; Paneque, M.; Petronilho, A.; Poveda, M. L.; del Río, D.; Serrano, O.; Carmona, E. *J. Am. Chem. Soc.* **2007**, *129*, 14130. (f) Buil, M. L.; Esteruelas, M. A.; Garcés, K.; Oliván, M.; Oñate, E. *J. Am. Chem. Soc.* **2007**, *129*, 10998. (g) Ruiz, J.; Perandones, B. F. *J. Am. Chem. Soc.* **2007**, *129*, 9298. (h) Esteruelas, M. A.; Fernández-Alvarez, F. J.; Oñate, E. *Organometallics* **2008**, *27*, 6236. (i) Gribble, M. W., Jr.; Ellman, J. A.; Bergman, R. G. *Organometallics* **2008**, *27*, 2152. (j) Song, G.; Su, Y.; Periana, R. A.; Crabtree, R. H.; Han, K.; Zhang, H.; Li, X. *Angew. Chem., Int. Ed.* **2010**, *49*, 912.

(7) The factors controlling the relative energies of C-bound **2** and N-bound **3** have been probed using DFT calculations: Häller, L. J. L.; Macgregor, S. A. *Eur. J. Inorg. Chem.* **2009**, 2000.

(8) Caddick, S.; Cloke, F. G. N.; Hitchcock, P. B.; de K. Lewis, A. K. *Angew. Chem., Int. Ed.* **2004**, *43*, 5824.

(9) (a) Mas-Marzá, E.; Poyatos, M.; Sanaú, M.; Peris, E. *Organometallics* **2004**, *23*, 323. (b) Mas-Marzá, E.; Poyatos, M.; Sanaú, M.; Peris, E. *Inorg. Chem.* **2004**, *43*, 2213. (c) Huynh, H. V.; Meier, N.; Pape, T.; Hahn, F. E. *Organometallics* **2006**, *25*, 3012. (d) Yen, S. K.; Koh, L. L.; Huynh, H. V.; Hor, T. S. A. *Dalton Trans.* **2007**, 3952. (e) Wang, X.; Chen, H.; Li, X. *Organometallics* **2007**, *26*, 4684. (f) Cabeza, J. A.; del Río, I.; Miguel, D.; Sánchez-Vega, M. G. *Angew. Chem., Int. Ed.* **2008**, *47*, 1920. (g) Cooke, C. E.; Jennings, M. C.; Katz, M. J.; Pomeroy, R. K.; Clyburne, J. A. C. *Organometallics* **2008**, *27*, 5777. (h) Han, Y.; Hong, Y.-T.; Huynh, H. V. *J. Organomet. Chem.* **2008**, *693*, 3159. (i) Ye, J.; Zhang, X.; Chen, W.; Shimada, S. *Organometallics* **2008**, *27*, 4166. (j) Liu, L.; Wang, F.; Shi, M. *Eur. J. Inorg. Chem.* **2009**, 1723. (k) Sabiah, S.; Lee, C.-S.; Hwang, W.-S.; Lin, I. J. B. *Organometallics* **2010**, *29*, 290. (l) Hu, Y.-C.; Tsai, C.-C.; Shih, W.-C.; Yap, G. P. A.; Ong, T.-G. *Organometallics* **2010**, *29*, 516.

Scheme 2

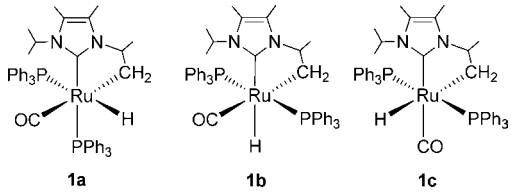

$[I^iPr_2Me_2H]Cl$. We propose that it is this $[I^iPr_2Me_2H]Cl$ that provides the HCl necessary to transform **1a** into **2**. In support of this, when a benzene solution of **1a** was heated at 70 °C in the presence of $[I^iPr_2Me_2H]Cl$, complete conversion to a mixture of **2**, **3**, and propene was observed over a period of 24 h. Alternative HCl sources, such as $[I^tBuH]Cl$ or $[NH_4]Cl$, were also shown to be capable of converting **1a** to the same mixture of products under similar conditions, although when a solution of HCl itself (4 M in dioxane) was used, decomposition of all the ruthenium species in solution was observed through elimination of imidazolium salt.

When the reaction of **1a** with $[I^iPr_2Me_2H]Cl$ at 70 °C was monitored over shorter time periods, isomerization to a mixture of **1a** and the previously reported complexes **1b** and **1c** in a 1:0.5:0.03 ratio was observed within 20 min,[4i,10] with no sign of either the C−N activated species **2** or its N-tautomer **3**. Complexes **1b** and **1c** exhibit a trans disposition of PPh_3 ligands and differ in the relative positions of the hydride and carbonyl ligands (Scheme 2). Of particular note is that **1c** and the C−N activated species **2** exhibit the same stereochemical orientation of NHC, PPh_3, and CO ligands. A reasonable postulate is therefore that **1a** first isomerizes to **1c**, which then undergoes C−N activation to afford **2**. In support of this, thermolysis of a solution of **1c** and $[I^tBuH]Cl$ in C_6D_6 for 1 h gave a mixture of **2** and **3** (ca. 50% conversion), whereas similar treatment of **1a** gave no more than 3% conversion to **2** and **3**. This implies that although **1a** can undergo rapid isomerization, the low equilibrium abundance of **1c** relative to **1a** results in significantly reduced formation of **2** and **3**.

Further experiments probed the reactivity of **1c**. First, C−N activation of **1c** (determined by monitoring the formation of propene by ^1H NMR spectroscopy) occurred at the same rate in the absence of a HCl source, although under these conditions a mixture of unidentified Ru-containing products was observed. This suggests that the role of HCl is simply to trap out the products **2** and **3** *after* cleavage of the C−N bond.[11] Second, heating solutions of **1c** and $[I^tBuH]Cl$ in the presence or absence of ca. 30 equiv of PPh_3 revealed no difference in the rate of either C−N activation or isomerization. Moreover, an equivalent reaction of **1c** and $[I^tBuH]Cl$ in the presence of ca. 30 equiv of $P(p\text{-tolyl})_3$ showed no incorporation of the tolylphosphine in the products. Therefore, neither the C−N activation nor the prior isomerization reactions involve phosphine dissociation.

Density Functional Theory (DFT) Calculations. We have undertaken DFT calculations to model the C−N activation process originating in **1a** and proceeding through **1c**. Experimentally, we have previously shown that isomerization of **1a** to **1c** proceeds through the five-coordinate agostic intermediate **5** (Scheme 3).[10] Labeling studies suggest that **5** is formed via protonation of a Ru(0) intermediate, **4**, which itself is derived from **1a** via C−H reductive elimination. **5** can be deprotonated by strong bases to give **1c**, a step which calculations indicate occurs via a novel C−H activation of a *non*agostic C−H bond. This mechanism is consistent with the isomerization of **1a** to **1c** occurring in the presence of $[I^iPr_2Me_2H]Cl$, which acts as a source of first a proton and then a strong base. A similar scheme could account for the formation of **1b** via deprotonation of an isomer of **5** where the H and CO ligands have exchanged positions.

Calculations on **1a**, **1b**, and **1c** showed **1a** to be most stable (relative energy 0.0 kcal/mol), followed by **1b** (E = +1.6 kcal/mol) and **1c** (E = +4.3 kcal/mol), and this ordering is in good qualitative agreement with the distribution of these three isomers in benzene at equilibrium. Computed geometries for **1a** and **1c** were also in good agreement with those determined experimentally.

Figure 1 shows computed reaction profiles for C−N activation in **1a** and **1c**. Although alternative mechanisms were considered,[12] ultimately this process was shown to entail a simple lengthening of the N1−C6 bond in the five-membered C−H activated ring. For isomer **1c** a transition state was located, $\mathbf{TS_{1c-6c}}$ (E = +24.4 kcal/mol), which shows significant elongation of both the N1−C6 distance (2.24 Å; cf. 1.49 Å in **1c**) and the bond to the metalated arm (Ru−C7 = 2.44 Å; cf. 2.25 Å in **1c**). The weaker Ru−C7 interaction results in a shortening of the Ru−H1 bond by 0.06 Å to 1.60 Å. The initial C−N cleavage product is the propene complex **6c** (E = +16.3 kcal/mol), and the shortening of the C6−C7 bond throughout this process reflects an increase in double bond character (**1c**, 1.55 Å; $\mathbf{TS_{1c-6c}}$, 1.40 Å; **6c**, 1.38 Å). **6c** also features a C2-metalated imidazole ligand with asymmetric C2−N1 and C2−N3 bonds (1.35 and 1.41 Å, respectively).

From **6c** the final observed C−N activation product, **2**, would be formed by protonation of N1 and displacement of propene by chloride. The fact that no propene adducts have been observed experimentally suggests that propene loss is facile, and this is also consistent with the long computed distances to the propene ligand in **6c** (Ru−C6 = 2.54 Å, Ru−C7 = 2.47 Å). The C−N cleavage step therefore controls the reactivity of the system, and for **1c** this occurs with an activation barrier of 20.1 kcal/mol.

C−N bond cleavage in **1a** proceeds via transition state $\mathbf{TS_{1a-6a}}$ (E = +29.9 kcal/mol) to give propene adduct **6a** (E = +17.7 kcal/mol). The geometric changes throughout this process are similar to those described above for **1c**, and the product complex **6a** again features a weakly bound propene ligand (Ru−C6 = 2.48 Å, Ru−C7 = 2.43 Å) and a shortened distance to the CO originally trans to the metalated arm (Ru−C8 = 1.88 Å (**1a**), 1.84 Å (**6a**)). The combination of experimental and computational results now allows us to propose the pathway shown in Scheme 4 for the conversion of **1a** to the C−N activated species **2**. The lower energy of **1a** means it will be the dominant species

Scheme 3

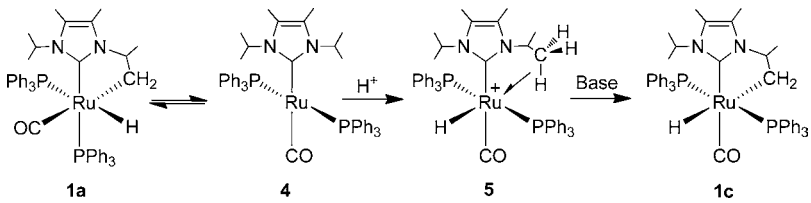

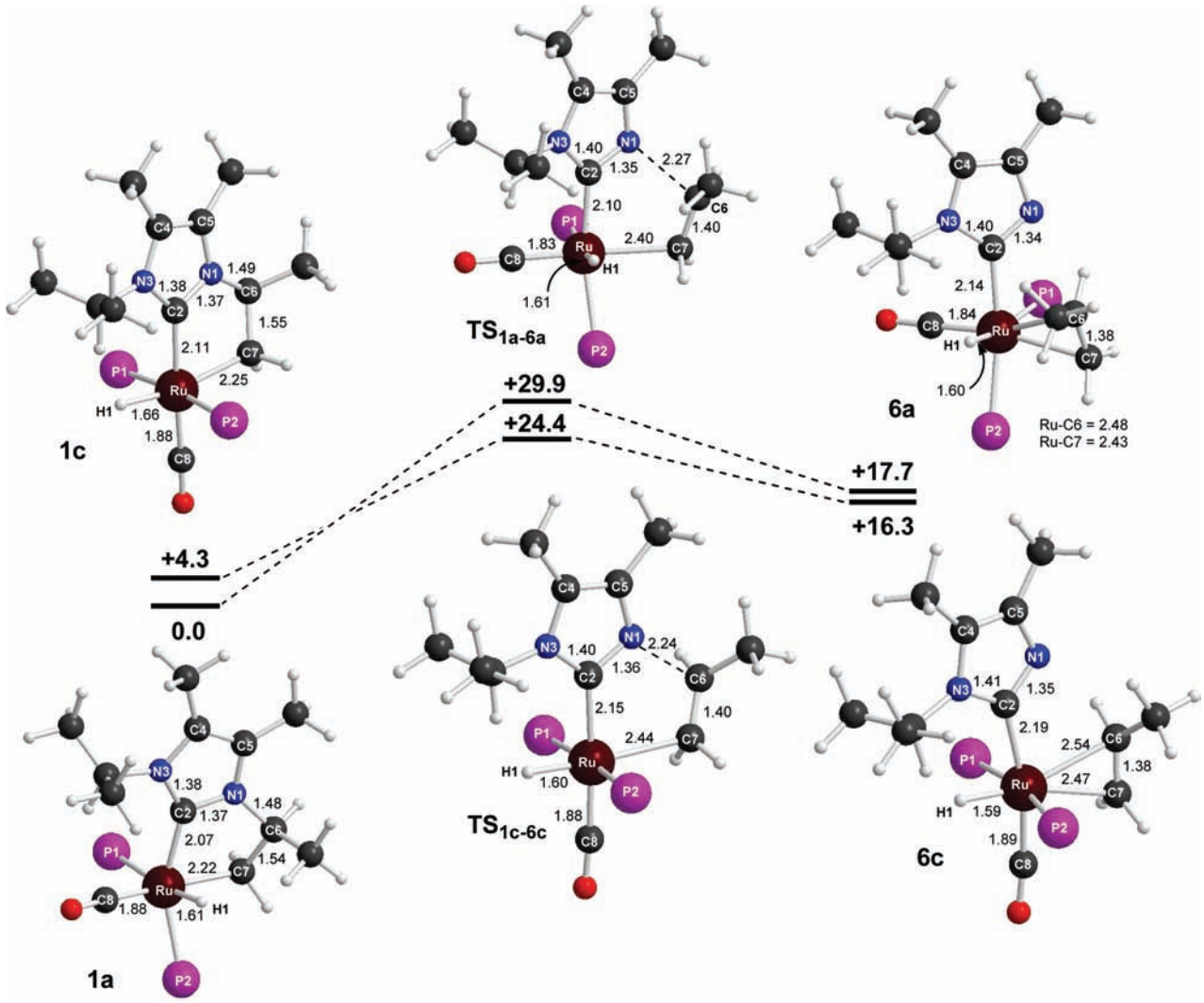

Figure 1. Computed reaction profiles (kcal/mol) for C−N activation in **1a** and **1c**. Selected distances are given in angstroms. Phenyl substituents on the phosphine ligands have been removed for clarity.

Scheme 4

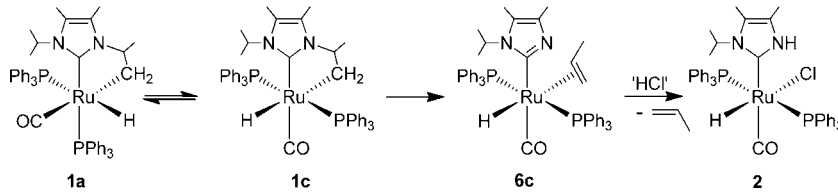

in solution; however, isomerization to **1c** allows the system to access the lower energy C−N cleavage pathway via $\mathbf{TS_{1c-6c}}$. C−N activation via this dual isomerization/cleavage process has an overall barrier (relative to **1a**) of 24.4 kcal/mol, significantly lower than direct reaction from **1a** (29.9 kcal/mol). The C2-metalated imidazole−propene complex **6c** loses propene and is trapped by HCl to generate **2** in the final step of the reaction.

To understand why C−N bond cleavage is so much easier in **1c** compared to **1a**, a range of model systems was considered in which the substituents at N1 (R), at the NHC C4/C5 backbone positions (R′), and in the phosphine (R″) were varied (see Table 1). In all cases the same trend was seen, with $\Delta E^{\ddagger}$(**1c**) being 8−10 kcal/mol lower than $\Delta E^{\ddagger}$(**1a**). This is particularly important with model 1 (R = R′ = R″ = H), where all significant ligand steric effects have been removed. The more facile C−N cleavage in isomer **1c** must therefore be primarily electronic in origin, and we suggest it arises from the unfavorable trans disposition of the high-trans-influence hydride and alkyl ligands present in **1c**. This causes an electronic destabilization that is relieved upon lengthening of the Ru−C7 bond in the C−N

(10) Häller, L. J. L.; Page, M. J.; Macgregor, S. A.; Mahon, M. F.; Whittlesey, M. K. *J. Am. Chem. Soc.* **2009**, *131*, 4604.
(11) When [I^{t}BuH]BF_4 was used instead of [I^{t}BuH]Cl to provide a source of HBF_4 rather than HCl, propene was generated but neither **2** nor **3** was formed.
(12) Alternative pathways based on initial formation of imidazolium via C−H reductive elimination proved inaccessible or very high in energy. In addition, introduction of an imidazolium cation as a proton source did not affect the computed C−N cleavage activation barriers. This latter observation is consistent with the fact that C−N activation of **1c** occurs at the same rate in the absence of a HCl source.

Table 1. Computed Energetics (kcal/mol) for C−N Activation with Different Models of **1a** and **1c**

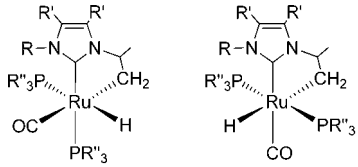

1a Model structure **1c** Model structure

model	1a	TS_{1a-6a}	$\Delta E^{\ddagger}$(1a)	1c	TS_{1c-6c}	$\Delta E^{\ddagger}$(1c)	$\Delta\Delta E^{\ddagger}$
(1) R = R′ = R″ = H	0.0	27.7	27.7	8.7	28.2	19.5	8.2
(2) R = Me; R′ = R″ = H	0.0	29.9	29.9	7.5	28.9	21.4	8.5
(3) R = ^{i}Pr; R′ = R″ = H	0.0	30.8	30.8	7.5	29.3	21.9	8.9
(4) R = ^{i}Pr; R′ = Me; R″ = H	0.0	31.2	31.2	8.4	30.1	21.8	9.4
(5) R = ^{i}Pr; R′ = Me; R″ = Ph	0.0	29.9	29.9	4.3	24.4	20.1	9.8

cleavage transition state. In **1a** CO is trans to the metalated arm, but the lower trans influence of this ligand means that the initial electronic destabilization is less significant and so results in a higher activation barrier.[13]

The results for model 1 show that, unlike the full experimental system (model 5), the *overall* barrier to C−N activation is lower for the direct reaction from **1a** (27.7 kcal/mol) rather than the isomerization/C−N cleavage route via **1c** (28.2 kcal/mol). The major difference between these two systems is in the relative energy of isomer **1c**. With model 1 **1c** lies 8.7 kcal/mol above **1a**, and this large difference outweighs the lower barrier for the C−N bond cleavage step found with **1c**. In model 5, the bulky PPh_3 ligands facilitate the initial isomerization and **1c** (with *trans*-PPh_3 ligands) is now only 4.3 kcal/mol above **1a** (with *cis*-PPh_3 ligands). As a result, the barrier for the isomerization/C−N cleavage route in the full system is 5.5 kcal/mol lower than that for the direct reaction from **1a**. The intermediate models 2−4 show that changes in the N3 and C4/C5 substituents cause only subtle changes in the relative energies of **1a** and **1c** and small increases in the C−N cleavage barriers for both isomers. In going from model 4 to model 5, the introduction of the full PPh_3 ligands stabilizes both transition states, suggesting that relief of steric strain also plays some role in promoting C−N activation in the full experimental systems.

In summary, two major factors come together to facilitate the isomerization/C−N cleavage process in **1a**: (i) the use of bulky PPh_3 ligands to facilitate isomerization to **1c** and (ii) the electronic activation of **1c** toward C−N cleavage by placing a high-trans-influence hydride ligand trans to the cyclometalated alkyl group.

Ancillary Ligand and NHC Substituent Effects on C−N Activation. The breadth of the C−N activation reaction was probed by studying the reactivity of analogues of **1** in which

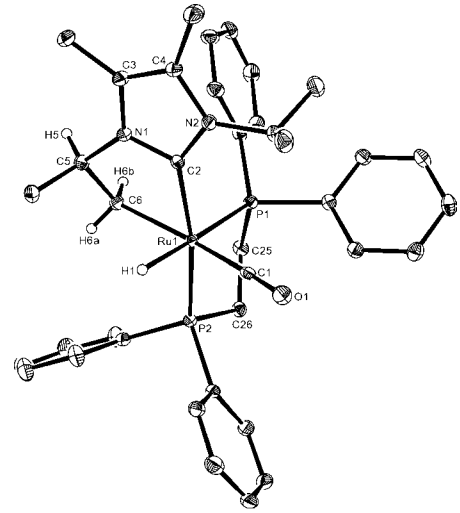

Figure 2. Molecular structure of $\mathbf{1a_{dppe}}$. Thermal ellipsoids are represented at 30% probability. All hydrogen atoms (except those on the activated carbene arm and Ru−H) are omitted for clarity. Selected bond lengths (Å) and angles (deg): Ru(1)−C(1), 1.864(2); Ru(1)−C(2), 2.064(2); Ru(1)−C(6), 2.208(2); Ru(1)−P(1), 2.3429(6); Ru(1)−P(2), 2.2978(7); P(1)−Ru(1)−P(2), 85.21(2); C(1)−Ru(1)−C(2), 96.69(9); C(2)−Ru(1)−C(6), 76.92(9); C(2)−Ru(1)−P(2), 169.02(6).

(i) the two PPh_3 groups were replaced by a chelating dppe ligand ($\mathbf{1_{dppe}}$), (ii) the NHC backbone substituents R′ were changed to Ph ($\mathbf{1_{iPr/Ph}}$) and H ($\mathbf{1_{iPr/H}}$), and (iii) the *N*-^{i}Pr substituents were changed to *N*-Et ($\mathbf{1_{Et/Me}}$) and *N*-^{t}Bu ($\mathbf{1_{tBu/Me}}$) groups. Scheme 5 shows the range of complexes that were investigated in the form of their **a** isomers.[4c,i]

1. C−N Bond Activation in $\mathbf{1a_{dppe}}$. The dppe complex $\mathbf{1a_{dppe}}$ was isolated in 68% yield following the reaction of Ru(dppe)(PPh_3)(CO)HCl with 2 equiv of $I^{i}Pr_2Me_2$ at 70 °C. The isomer **a** geometry was confirmed by the appearance of large and small phosphorus couplings to the single hydride resonance at δ −5.8 (J_{HP} = 108, 19 Hz) and the carbenic carbon signal at δ 190 (J_{CP} = 85, 10 Hz), as well as by an X-ray crystal structure (Figure 2). In comparison to the structure of **1a**,[4i] the presence of the dppe ligand results in a much more acute P−Ru−P angle ($\mathbf{1a_{dppe}}$, 85.21(2)°; **1a**, 102.152(15)°) and shorter Ru−P bond lengths ($\mathbf{1a_{dppe}}$, 2.2978(7), 2.3429(6) Å; **1a**, 2.3445(4), 2.4357(4) Å).

In contrast to **1a**, thermolysis of a benzene solution of $\mathbf{1a_{dppe}}$ and [I^{t}BuH]Cl at 70 °C for several days gave no C−N activated products. In this case, a reaction path involving a *trans*-phosphine isomer equivalent to **1c** is not accessible due to the presence of the chelating dppe ligand. However, the necessary *trans*-H−Ru−alkyl arrangement can be achieved in isomer $\mathbf{1d_{dppe}}$, in which the H and CO have exchanged positions compared to those in $\mathbf{1a_{dppe}}$. DFT calculations on C−N cleavage in $\mathbf{1d_{dppe}}$ predict a barrier of 26.2 kcal/mol, somewhat higher than that computed for **1a**, but potentially still accessible at higher temperatures. Indeed, heating $\mathbf{1a_{dppe}}$ at 120 °C for 24 h

Scheme 5

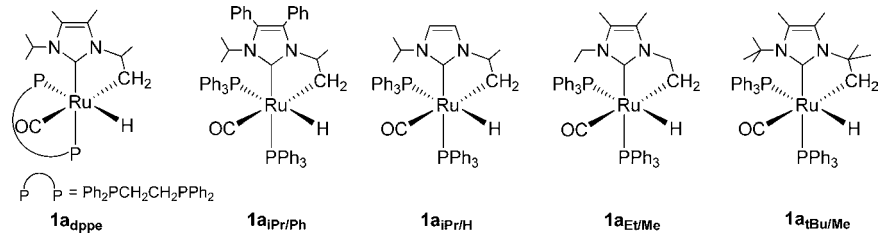

Scheme 6

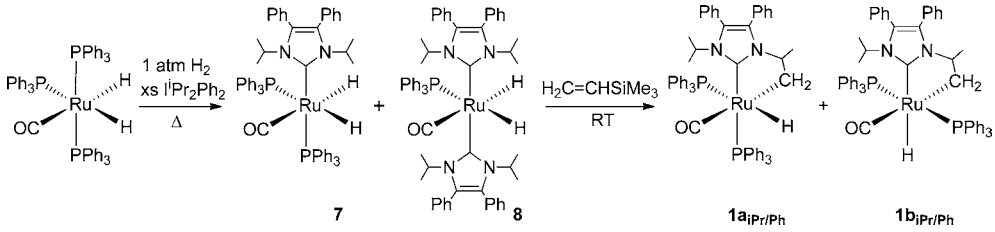

in the presence of [I^{t}BuH]Cl did lead to C−N activation with formation of both propene and 1-isopropyl-4,5-dimethylimidazole, although no clearly identifiable ruthenium-containing species were formed. The computed barrier for direct C−N cleavage in $\mathbf{1a_{dppe}}$ had a much higher computed barrier of 32.2 kcal/mol, and this re-emphasizes the role of the *trans*-hydride ligand in promoting this process.

2. C−N Bond Activation in $\mathbf{1}^{i}_{Pr/Ph}$ and $\mathbf{1}^{i}_{Pr/H}$. The attempted synthesis of $\mathbf{1}^{i}_{Pr/Ph}$ via reaction of $Ru(PPh_3)_3(CO)HCl$ with an excess of the free carbene $I^iPr_2Ph_2$ at 70 °C formed a mixture of $\mathbf{1}^{i}_{Pr/Ph}$, $Ru(I^iPr_2Ph_2)(PPh_3)_2(CO)H_2$ (**7**), and $Ru(I^iPr_2Ph_2)_2(PPh_3)(CO)H_2$ (**8**), as well as propene and 1-isopropyl-4,5-diphenylimidazole. When the reaction was performed under 1 atm of H_2, only **7** and **8** were formed.[14] Isolation of **7** followed by reaction with the hydrogen acceptor $CH_2{=}CHSiMe_3$ for several days at room temperature afforded $\mathbf{1}^{i}_{Pr/Ph}$ in 63% isolated yield (Scheme 6). ^1H and $^{31}P\{^1H\}$ NMR spectroscopy revealed that $\mathbf{1}^{i}_{Pr/Ph}$ was present in solution as a 3:2 mixture of the two isomers $\mathbf{1a}^{i}_{Pr/Ph}$ and $\mathbf{1b}^{i}_{Pr/Ph}$. Thus, the hydride region of the proton NMR spectrum exhibited a doublet of doublets for $\mathbf{1a}^{i}_{Pr/Ph}$ at δ −7.6 (J_{HP} = 103, 28 Hz) and a triplet for $\mathbf{1b}^{i}_{Pr/Ph}$ at δ −7.3 (J_{HP} = 24 Hz). As expected, the $^{31}P\{^1H\}$ NMR spectrum showed two doublet resonances at δ 56.7 and 36.5 (J_{PP} = 16 Hz) arising from $\mathbf{1a}^{i}_{Pr/Ph}$ and an AB pattern for $\mathbf{1b}^{i}_{Pr/Ph}$ centered at δ 59.7.

The X-ray crystal structure of the major isomer $\mathbf{1a}^{i}_{Pr/Ph}$ (Figure 3) revealed the expected distorted octahedral geometry. The metrical parameters of $\mathbf{1a}^{i}_{Pr/Ph}$ were very similar to those of **1a**, showing that backbone phenyl groups have only a minimal impact on structure.

Thermolysis of the isomeric mixture of $\mathbf{1a}^{i}_{Pr/Ph}/\mathbf{1b}^{i}_{Pr/Ph}$ with [I^{t}BuH]Cl in benzene at 70 °C for 6 h gave a mixture of $\mathbf{2}^{i}_{Pr/Ph}$ and the N-bound tautomer $\mathbf{3}^{i}_{Pr/Ph}$ (Scheme 7).[15] Some of the starting material remained, although all of this disappeared over a period of 24 h.[16] In an effort to provide at least a qualitative order to the influence of the backbone groups on C−N activation, benzene solutions of **1a** and $\mathbf{1a}^{i}_{Pr/Ph}/\mathbf{1b}^{i}_{Pr/Ph}$ were heated with 2 equiv of [I^{t}BuH]Cl at 70 °C side by side over a period of ca. 60 h. Depletion of the starting hydride signal and the appearance of propene were measured intermittently by proton NMR against an internal standard of ferrocene and found to follow the order $\mathbf{1a}^{i}_{Pr/Ph} > \mathbf{1a}$.

When C−N activation in $\mathbf{1}^{i}_{Pr/Ph}$ was modeled with DFT calculations as for $\mathbf{1}^{i}_{Pr/Me}$ above, isomer $\mathbf{1a}^{i}_{Pr/Ph}$ was found to be the most stable form, in agreement with the experimental observations. The lowest energy C−N activation transition state is again accessed through isomer **c** (E = +4.0 kcal/mol) and proceeds with an overall barrier of 21.4 kcal/mol, lower than found for $\mathbf{1}^{i}_{Pr/Me}$ (+24.4 kcal/mol) and therefore consistent with the more rapid reaction seen for the former.

Experimental studies on $\mathbf{1}^{i}_{Pr/H}$, which has only hydrogen atoms at the backbone C4 and C5 positions, revealed behavior quite different from that of $\mathbf{1}^{i}_{Pr/Ph}$ and $\mathbf{1}^{i}_{Pr/Me}$. First, $\mathbf{1}^{i}_{Pr/H}$ has been shown previously to exist in solution as the **b** isomer.[10] When it was heated with [I^{t}BuH]Cl at 70 °C for 48 h, the formation of both propene and 1-isopropylimidazole was observed, indicating that C−N activation was still occurring, although only trace amounts of the corresponding C- and N-bound ruthenium products $\mathbf{2}^{i}_{Pr/H}$ and $\mathbf{3}^{i}_{Pr/H}$ were formed.[17] The predominant ruthenium-containing product was now $Ru(PPh_3)_3(CO)H_2$, implying that carbene loss becomes a major pathway when R′ = H. DFT calculations confirm that isomer **1b** is more stable than **1a** (by 0.8 kcal/mol); however, the computed barrier via the standard isomerization/C−N cleavage

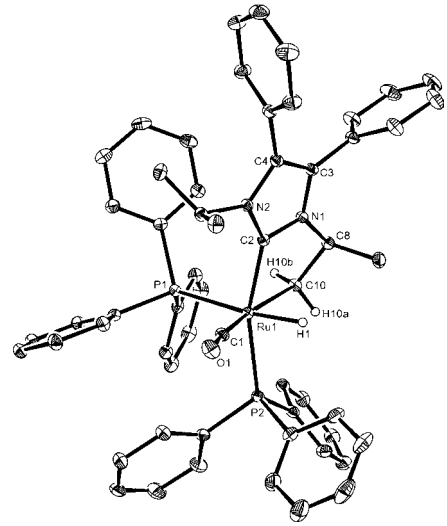

Figure 3. Molecular structure of $\mathbf{1a}^{i}_{Pr/Ph}$. Thermal ellipsoids are represented at 30% probability. Solvent and all hydrogen atoms (except those on the activated carbene arm and Ru−H) are omitted for clarity. Selected bond lengths (Å) and angles (deg): Ru(1)−C(1), 1.8640(18); Ru(1)−C(2), 2.0668(16); Ru(1)−C(10), 2.2058(16); Ru(1)−P(1), 2.4124(4); Ru(1)−P(2), 2.3457(4); P(1)−Ru(1)−P(2), 102.520(15); C(1)−Ru(1)−C(2), 95.56(7); C(2)−Ru(1)−C(10), 76.94(6); C(2)−Ru(1)−P(2), 161.80(5).

(13) For the same reasons, C−N cleavage in **1b** (where CO is also trans to alkyl) involves a high barrier of +27.3 kcal/mol, while C−N activation in a fourth isomer, **1d** (E = +7.2 kcal/mol), related to **1a** via exchange of H and CO ligands, leads to a lower barrier of only 22.8 kcal/mol.

(14) The X-ray structure of **7** is given in the Supporting Information.

(15) The C−N activated complex $\mathbf{2}^{i}_{Pr/Ph}$ was identified by comparison of its NMR spectrum to that of **2**, with the Ru−H (δ −14.0) and N−H (δ 11.7) proton resonances appearing at chemical shifts very similar to those of **2** (Ru−H, δ −14.0; N−H, δ 10.2). The identity of the N-bound tautomer $\mathbf{3}^{i}_{Pr/Ph}$ was confirmed by an independent synthesis involving the reaction of $Ru(PPh_3)_3(CO)HCl$ with 1-isopropyl-4,5-diphenylimidazole (see the Supporting Information).

(16) The formation of $\mathbf{2}^{i}_{Pr/Ph}$ and $\mathbf{3}^{i}_{Pr/Ph}$ was accompanied by two other Ru−phosphine species, a hydride-containing complex, **9**, and a non-hydridic compound, **10**. Prolonged heating (≥72 h) afforded **10** as the major reaction product. Spectroscopic and structural details for **10**, which contains a C−H activated phenyl group on the backbone of the NHC ligand, are provided in the Supporting Information.

(17) The reaction of $Ru(PPh_3)_3(CO)HCl$ and *N*-isopropylimidazole was used for the independent synthesis of $\mathbf{3}^{i}_{Pr/H}$. See the Supporting Information.

Scheme 7

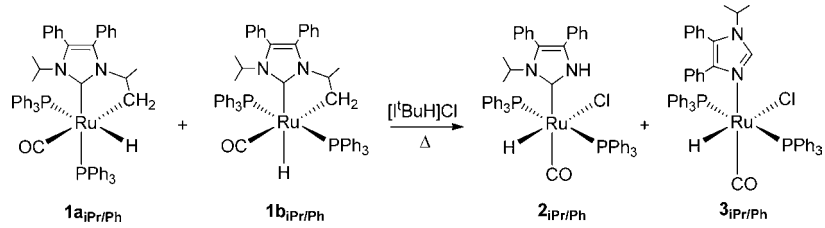

process is only +24.1 kcal/mol (relative to **1b**). This would be inconsistent with the slower reaction of $\mathbf{1}_{\mathbf{^iPr/H}}$ compared to $\mathbf{1}_{\mathbf{^iPr/Me}}$. This result, in combination with the different behavior of $\mathbf{1}_{\mathbf{^iPr/H}}$ seen experimentally, suggests that the detailed mechanism of C−N activation may well be different in this case.

3. C−N Bond Activation in $\mathbf{1}_{\mathbf{Et/Me}}$ and $\mathbf{1}_{\mathbf{^tBu/Me}}$. The influence of the N-substituent was established by turning to the *N*-ethyl complex $\mathbf{1}_{\mathbf{Et/Me}}$, which also exists in solution as the **b** isomer. When $\mathbf{1b}_{\mathbf{Et/Me}}$ was heated in the presence of [I^{t}BuH]Cl, <10% conversion to the C- and N-bound products $\mathbf{2}_{\mathbf{Et/Me}}$ and $\mathbf{3}_{\mathbf{Et/Me}}$ was found even after one week at 70 °C.[18] DFT calculations found isomers **1a** and **1b** to be almost equienergetic in this case, while the computed overall barrier to C−N activation via $\mathbf{TS}_{\mathbf{1c-6c}}$ was 25.6 kcal/mol. This higher barrier is consistent with the lower reactivity seen for $\mathbf{1}_{\mathbf{Et/Me}}$ compared to either $\mathbf{1}_{\mathbf{^iPr/Me}}$ or $\mathbf{1}_{\mathbf{^iPr/Ph}}$ and reflects the nature of the alkene being formed; hyperconjugation effects should help stabilize the incipient propene moiety in $\mathbf{TS}_{\mathbf{1c-6c}}$ derived from $\mathbf{1}_{\mathbf{^iPr/Me}}$ (or $\mathbf{1}_{\mathbf{^iPr/Ph}}$), but no such stabilization is available in the equivalent transition state involving ethene formation from $\mathbf{1}_{\mathbf{Et/Me}}$.

The *N*-^{t}Bu analogue, $\mathbf{1}_{\mathbf{^tBu/Me}}$, would help substantiate this idea, as the formation of 2-methylpropene should further favor C−N activation. Although this species could not be accessed experimentally, calculations were able to define a barrier of 21.3 kcal/mol relative to the most stable isomer $\mathbf{1a}_{\mathbf{^tBu/Me}}$, significantly lower than for either $\mathbf{1a}_{\mathbf{^iPr/Me}}$ (24.4 kcal/mol) or $\mathbf{1a}_{\mathbf{Et/Me}}$ (25.6 kcal/mol).

Conclusions

A combination of experimental studies and DFT calculations has been used to show that C−N bond activation of the N-heterocyclic carbene ligand in the C−H activated complex Ru(I^{i}Pr$_2$Me$_2$)′(PPh$_3$)$_2$(CO)H (I^{i}Pr$_2$Me$_2$ = 1,3-diisopropyl-4,5-dimethylimidazol-2-ylidene) involves initial isomerization to a *trans*-phosphine isomer, **1c**, in which the hydride ligand is trans to the metalated carbene arm. C−N cleavage then gives an intermediate propene complex that features a C2-bound imidazole ligand. Under the reaction conditions this species reacts with imidazolium chloride as a source of HCl to afford the experimentally observed C−N activated product **2** (Scheme 1).

C−N activation in **1c** is promoted by an electronic destabilization that arises from the trans arrangement of high-trans-influence hydride and alkyl ligands. This is relieved in the transition state by C−N bond cleavage within the five-membered C−H activated ring. The preliminary isomerization step is also promoted by bulky PPh$_3$ ligands that facilitate a *trans*-phosphine geometry. We have also established that C−N cleavage is promoted by Ph substituents at the backbone positions of the NHC and by more highly substituted alkyl substituents on the N atoms of the imidazolylidene rings.

Our study shows that *N*-alkyl NHC ligands that undergo intramolecular C−H activation may be particularly susceptible to irreversible C−N activation. In addition to forming the cyclometalated ring that is necessary for alkene formation, this process also produces hydride-containing species, and this high-trans-influence ligand can promote the C−N cleavage reaction. Given the propensity of NHC ligands to intramolecular C−H activation on a wide varietry of metal centers[3,4] and the continuing interest of many groups in using bulky carbenes to stabilize low-coordinate complexes,[19] our findings would suggest that many more examples of C−N activation will be forthcoming.

Experimental Section

General Comments. All manipulations were carried out using standard Schlenk, high-vacuum, and glovebox techniques. Solvents were purified using an MBraun SPS solvent system (toluene, Et$_2$O, hexane) or under a nitrogen atmosphere from sodium benzophenone ketyl (benzene) or Mg/I$_2$ (EtOH). Deuterated solvents (Fluorochem) were vacuum transferred from potassium (C$_6$D$_6$) or CaH$_2$ (CD$_2$Cl$_2$). Ru(I^{i}Pr$_2$Me$_2$)′(PPh$_3$)$_2$(CO)H (**1**),[1i,5] Ru(dppe)(PPh$_3$)(CO)HCl,[20] Ru(PPh$_3$)$_3$(CO)HCl,[21] Ru(IEt$_2$Me$_2$)′(PPh$_3$)$_2$(CO)H ($\mathbf{1}_{\mathbf{Et/Me}}$),[4c] I^{i}Pr$_2Me_2$,[22] and [I^{i}Pr$_2Ph_2$H]BF$_4$[23] were prepared according to the literature. NMR spectra were recorded on Bruker Avance 400 and 500 MHz NMR spectrometers at 298 K with ^{1}H and ^{13}C{^{1}H} spectra referenced as follows: C$_6$D$_6$ at δ 7.15 (^{1}H), δ 128.0 (^{13}C); CD$_2$Cl$_2$ at δ 5.32 (^{1}H), δ 54.0 (^{13}C). ^{31}P{^{1}H} NMR chemical shifts were referenced externally to 85% H$_3$PO$_4$ (δ 0.0). IR spectra were recorded on a Nicolet Nexus FTIR spectrometer. Mass spectrometry was undertaken using a micrOTOF electrospray time-of-flight (ESI-TOF) mass spectrometer (Bruker Daltonik GmbH). Elemental analyses were performed by Elemental Microanalysis Ltd., Okehampton, Devon, U.K.

Ru(I^{i}Pr$_2$Me$_2$)′(dppe)(CO)H ($\mathbf{1a}_{\mathbf{dppe}}$). A solution of Ru(dppe)(PPh$_3$)(CO)HCl (588 mg, 0.711 mmol) and I^{i}Pr$_2$Me$_2$ (277 mg, 1.536 mmol) in toluene (10 mL) was heated at 70 °C overnight to yield a white precipitate of the imidazolium salt [I^{i}Pr$_2$Me$_2$H]Cl and a pale yellow solution. The solution was filtered, and hexane (50 mL) was added to the eluent to precipitate a beige solid of the product, which was filtered, washed with hexane (2 × 3 mL), and dried in vacuo. Yield: 345 mg, 68%. ^{1}H NMR (500 MHz, C$_6$D$_6$): δ 8.03 (t, 2H, J = 8.5 Hz, C$_6$*H*$_5$), 7.99 (t, 2H, J = 8.5 Hz, C$_6$*H*$_5$), 7.77 (t, 2H,

(18) Under more forcing conditions (60 h, 95 °C) formation of the N-bound tautomer $\mathbf{3}_{\mathbf{Et/Me}}$ was achieved. The identity of the product was confirmed by an X-ray crystal structure following an independent synthesis from Ru(PPh$_3$)$_3$(CO)HCl with 1-ethyl-4,5-dimethylimidazole. See the Supporting Information.

(19) See, for example: (a) Arduengo, A. J., III; Gamper, S. F.; Calabrese, J. C.; Davidson, F. *J. Am. Chem. Soc.* **1994**, *116*, 4391. (b) Yamashita, M.; Goto, K.; Kawashima, T. *J. Am. Chem. Soc.* **2005**, *127*, 7294. (c) Laitar, D. S.; Müller, P.; Gray, T. G.; Sadighi, J. P. *Organometallics* **2005**, *24*, 4503. (d) van der Eide, E. F.; Romero, P. E.; Piers, W. E. *J. Am. Chem. Soc.* **2008**, *130*, 4485. (e) Miyazaki, S.; Koga, Y.; Matsumoto, T.; Matsubara, K. *Chem. Commun.* **2010**, *46*, 1932.

(20) Santos, A.; López, J.; Montoya, J.; Noheda, P.; Romero, A.; Echavarren, A. M. *Organometallics* **1994**, *13*, 3605.

(21) Ahmad, N.; Levison, J. J.; Robinson, S. D.; Uttley, M. F. *Inorg. Synth.* **1974**, *15*, 45.

(22) Kühn, N.; Kratz, T. *Synthesis* **1993**, 561.

(23) Chianese, A. R.; Kovacevic, A.; Zeglis, B. M.; Faller, J. W.; Crabtree, R. H. *Organometallics* **2004**, *23*, 2461.

J = 8.5 Hz, C_6H_5), 7.15 (m, 4H, C_6H_5), 7.10−6.90 (m, 10H, C_6H_5), 5.63 (sept, 1H, $^3J_{HH}$ = 7.0 Hz, C*H*(CH_3)$_2$), 3.92 (m, 1H, C*H*(CH_3)(CH_2)), 2.36 (m, 2H, PCH_2), 2.09 (m, 1H, PCH_2), 1.95 (m, 1H, PCH_2), 1.78 (s, 3H, NCCH_3), 1.70 (s, 3H, NCCH_3), 1.45 (d, 3H, $^3J_{HH}$ = 6.3 Hz, CH(CH_3)), 1.38 (d, 3H, $^3J_{HH}$ = 7.0 Hz, CH(CH_3)), 0.92 (d, 3H, $^3J_{HH}$ = 7.0 Hz, CH(CH_3)), 0.71 (m, 1H, CH*H*′), 0.30 (br t, 1H, J = 10.2 Hz, C*H*H′), −5.78 (dd, 1H, $^2J_{HP}$ = 107.9 Hz, $^2J_{HP}$ = 19.2 Hz, Ru*H*). ^{31}P{^{1}H} NMR (202 MHz, C_6D_6): δ 76.8 (d, $^2J_{PP}$ = 5.0 Hz), 58.5 (d, $^2J_{PP}$ = 5.0 Hz). ^{13}C{^{1}H} NMR (125 MHz, C_6D_6): δ 208.5 (dd, $^2J_{CP}$ = 9 Hz, $^2J_{CP}$ = 5 Hz, *C*O), 189.8 (dd, $^2J_{CP}$ = 85 Hz, $^2J_{CP}$ = 10 Hz, N*C*N), 143.1 (d, J_{CP} = 22 Hz, PC_6H_5), 140.8 (d, J_{CP} = 34 Hz, PC_6H_5), 138.3 (d, J_{CP} = 38 Hz, PC_6H_5), 136.2 (d, J_{CP} = 23 Hz, PC_6H_5), 133.3 (d, J_{CP} = 10 Hz, PC_6H_5), 132.9 (d, J_{CP} = 12 Hz, PC_6H_5), 132.6 (d, J_{CP} = 11 Hz, PC_6H_5), 129.2 (s, PC_6H_5), 128.8 (s, PC_6H_5), 128.7 (s, PC_6H_5), 124.0 (s, N*C*CH$_3$), 122.5 (s, N*C*CH$_3$), 58.8 (d, J_{CP} = 6 Hz, *C*H(CH$_3$)), 54.0 (s, *C*H(CH$_3$)$_2$), 30.4 (dd, J_{CP} = 22 Hz, J_{CP} = 18 Hz, P*C*H$_2$), 28.1 (dd, J_{CP} = 24 Hz, J_{CP} = 21 Hz, P*C*H$_2$), 22.8 (s, CH(*C*H$_3$)), 21.9 (s, CH(*C*H$_3$)), 21.8 (s, CH(*C*H$_3$)), 20.5 (dd, $^2J_{CP}$ = 9 Hz, $^2J_{CP}$ = 7 Hz, Ru*C*H$_2$), 11.0 (s, NC*C*H$_3$), 9.6 (s, NC*C*H$_3$). IR (C_6H_6, cm^{-1}): 1885 (ν_{CO}). Anal. Found (Calcd) for $C_{38}H_{44}N_2OP_2Ru$: C, 64.10 (64.48); H, 6.09 (6.27); N, 3.94 (3.96).

Ru(I^{i}Pr$_2$Ph$_2$)′(PPh$_3$)$_2$(CO)H (1a$_{iPr/Ph}$/1b$_{iPr/Ph}$). A benzene (10 mL) solution of Ru(I^{i}Pr$_2$Ph$_2$)(PPh$_3$)$_2$(CO)H$_2$[24] (**7**; 90 mg, 0.094 mmol) and H_2C═CHSiMe$_3$ (200 μL, 1.36 mmol) in benzene was stirred at room temperature for 72 h. The volatiles were removed under vacuum, and the residue was washed with hexane (2 × 3 mL) to yield a white precipitate of **1a$_{iPr/Ph}$** and **1b$_{iPr/Ph}$** (57 mg, 63%). Recrystallization of the precipitate from benzene/hexane allowed **1a$_{iPr/Ph}$** to be isolated. ^{1}H NMR (500 MHz, C_6D_6): δ 7.72 (m, 6H, C_6H_5), 7.49 (t, 6H, J = 8.1 Hz, C_6H_5), 7.17 (d, 2H, J = 8.1 Hz, C_6H_5), 7.10−6.93 (m, 22H, C_6H_5), 6.88 (m, 4H, C_6H_5), 5.59 (sept, 1H, $^3J_{HH}$ = 7.0 Hz, C*H*(CH_3)$_2$), 4.88 (m, 1H, C*H*(CH_3)(CH_2)), 2.19 (m, 1H, CH*H*′), 1.71 (d, 3H, $^3J_{HH}$ = 7.0 Hz, CH(CH_3)), 1.15 (d, 3H, $^3J_{HH}$ = 6.2 Hz, CH(CH_3)), 0.60 (br t, 1H, J = 6.7 Hz, C*H*H′), 0.23 (d, 3H, $^3J_{HH}$ = 7.0 Hz, CH(CH_3)), −7.55 (dd, 1H, $^2J_{HP}$ = 103.4 Hz, $^2J_{HP}$ = 28.2 Hz, Ru*H*). ^{31}P{^{1}H} NMR (202 MHz, C_6D_6): δ 56.7 (d, $^2J_{PP}$ = 16.1 Hz), 36.5 (d, $^2J_{PP}$ = 16.1 Hz). ^{13}C{^{1}H} NMR (125 MHz, C_6D_6): δ 206.7 (dd, $^2J_{CP}$ = 13 Hz, $^2J_{CP}$ = 6 Hz, *C*O), 191.0 (dd, $^2J_{CP}$ = 83 Hz, $^2J_{CP}$ = 10 Hz, N*C*N), 139.8 (C_6H_5), 139.6 (d, J_{CP} = 9 Hz, PC_6H_5), 135.2 (d, J_{CP} = 11 Hz, PC_6H_5), 134.6 (s, C_6H_5), 134.5 (s, C_6H_5), 132.4 (s, N*C*C_6H_5), 131.7 (s, N*C*C_6H_5), 130.4 (s, C_6H_5), 128.9 (s, PC_6H_5), 128.3 (d, J_{CP} = 8 Hz, PC_6H_5), 128.1 (s, C_6H_5), 128.0 (s, C_6H_5), 58.9 (s, *C*H(CH$_3$)), 55.5 (s, *C*H(CH$_3$)$_2$), 25.5 (s, CH(*C*H$_3$)), 23.8 (t, $^2J_{CP}$ = 7 Hz, Ru*C*H$_2$), 22.0 (s, CH(*C*H$_3$)), 21.9 (s, CH(*C*H$_3$)). IR (C_6H_6, cm^{-1}): 1889 (ν_{CO}). Anal. Found (Calcd) for $C_{58}H_{55}N_2OP_2Ru\cdot C_6H_6$: C, 73.81 (74.11); H, 5.82 (5.93); N, 2.65 (2.70).

X-ray Crystallography. Single crystals of compounds **1a$_{dppe}$** and **1a$_{iPr/Ph}$** were analyzed at 150 K using Mo Kα radiation on a Nonius Kappa CCD diffractometer. Details of the data collections, solutions, and refinements are given in Table 2. The structures were solved using SHELXS-97[25] and refined using full-matrix least-squares analysis in SHELXL-97.[25] Refinements were generally straightforward with the following exceptions and points of note. H1, H5, H6a, and H6B in **1a$_{dppe}$** were located and refined at distances of 1.6 Å (for H1), and 0.9 Å (for the latter three hydrogens) from the relevant parent atoms. The asymmetric unit in **1a$_{iPr/Ph}$** contains one molecule of benzene in addition to one molecule of the ruthenium complex. As for **1a$_{dppe}$**, the hydride (H1) was located and refined at 1.6 Å from Ru1. H10a and H10b were ultimately included at calculated positions proximate to those evident in the penultimate difference Fourier electron density map. Crystallographic data for compounds **1a$_{dppe}$** and **1a$_{iPr/Ph}$** have been deposited with the Cambridge Crystallographic Data Centre as Supplementary Publications CCDC 756039 and 756040. Copies of the data can be obtained free of charge on application to CCDC, 12 Union Rd., Cambridge CB2 1EZ, U.K. [fax, (+44) 1223 336033; e-mail, deposit@ccdc.cam.ac.uk].

Table 2. Crystal Data and Structure Refinement for Compounds **1a$_{dppe}$** and **1a$_{iPr/Ph}$**

	1a$_{dppe}$	**1a$_{iPr/Ph}$**
empirical formula	$C_{38}H_{44}N_2OP_2Ru$	$C_{64}H_{60}N_2OP_2Ru$
fw	707.76	1036.15
cryst syst	triclinic	triclinic
space group	$P\bar{1}$	$P\bar{1}$
a (Å)	11.2630(2)	10.1400(1)
b (Å)	12.6030(2)	13.6920(2)
c (Å)	12.7410(2)	19.2510(3)
α (deg)	99.643(1)	81.982(1)
β (deg)	94.862(1)	86.649(1)
γ (deg)	104.420(1)	84.854(1)
U (Å^3)	1711.56(5)	2633.09(6)
Z	2	2
D_c (g cm^{-3})	1.373	1.307
μ (mm^{-1})	0.584	0.403
F(000)	736	1080
cryst size (mm)	0.30 × 0.25 × 0.25	0.30 × 0.25 × 0.25
θ min, max for data collection (deg)	3.88, 30.00	3.79, 27.53
index ranges	$-15 \le h \le +15$, $-17 \le k \le +17$, $-17 \le l \le +17$	$-13 \le h \le +13$, $-17 \le k \le +17$, $-24 \le l \le +25$
no. of reflns collected	37121	51926
no. of independent reflns, R_{int}	9889, 0.0861	11986, 0.0349
no. of reflns obsd (>2σ)	7010	10606
data completeness	0.993	0.989
abs correction	multiscan	multiscan
max, min transmission	0.89, 0.79	0.908, 0.852
no. of data/restraints/params	9889/4/416	11986/1/640
goodness-of-fit on F^2	0.984	1.074
final R1, wR2 [I > 2σ(I)]	0.0430, 0.0837	0.0291, 0.0713
final R1, wR2 (all data)	0.0797, 0.0939	0.0364, 0.0761
largest diff peak, hole (e Å^{-3})	0.597, −0.919	0.484, −0.574

Computational Details. DFT calculations were run with Gaussian 03 (revision D.01)[26] using the BP86 functional. Ru and P centers were described with the Stuttgart RECPs and associated basis sets,[27] with added d-orbital polarization on P.[28] 6-31G** basis sets were used for all other atoms.[29] All stationary points were fully characterized via analytical frequency calculations as either minima (all positive eigenvalues) or transition states (one imaginary eigenvalue), and IRC calculations and subsequent geometry optimizations were used to confirm the minima linked by each transition state. Reported energies include a correction for zero-point energies.

The following protocol was adopted to ensure that the lowest energy conformations were located for each stationary point. For each initial structure (derived from experiment or built from chemical intuition) a molecular dynamics (MD) simulation was

(24) See the Supporting Information.

(25) Sheldrick, G. M. *Acta. Crystallogr.* **1990**, *467−473*, A46. Sheldrick, G. M. *SHELXL-97, a computer program for crystal structure refinement*; University of Göttingen: Göttingen, Germany, 1997.

(26) Frisch, M. J.; et al. *Gaussian 03*, revision D.01; Gaussian, Inc.: Wallingford, CT, 2004.

(27) Andrae, D.; Häussermann, U.; Dolg, M.; Stoll, H.; Preuss, H. *Theor. Chim. Acta* **1990**, *77*, 123.

(28) Höllwarth, A.; Böhme, M.; Dapprich, S.; Ehlers, A. W.; Gobbi, A.; Jonas, V.; Köhler, K. F.; Stegmann, R.; Veldkamp, A.; Frenking, G. *Chem. Phys. Lett.* **1993**, *208*, 237.

(29) (a) Hehre, W. J.; Ditchfield, R.; Pople, J. A. *J. Chem. Phys.* **1972**, *56*, 2257. (b) Hariharan, P. C.; Pople, J. A. *Theor. Chim. Acta* **1973**, *28*, 213.

performed using the Tinker program[30] and the MM3 force field. These runs allowed movement of the hydrocarbyl substituents on the phosphine and NHC ligands, with all other bonds being fixed. MD simulations were run for 1 ns with a 1 fs time step in an NVT ensemble, with coordinates being collected every picosecond to generate 1000 structures. The trajectories were propagated using the modified Beeman integration algorithm,[31] and a Berendsen thermostat[32] was used to keep the temperature around 1000 K. We found this relatively high temperature was needed to span the conformational space in the most efficient way. The 1000 generated structures were then optimized with the MM3 force field with the same geometry constraints as above. Energetically unique structures (typically between 15 and 60 conformations for each stationary point) were then selected for optimization at the DFT level using the "opt=loose" option in G03 and an SCF convergence of 10^{-6} au. The lowest energy structure and any others within approximately 1 kcal/mol (typically up to three structures) were then optimized with regular convergence criteria and characterized via frequency analyses. Sampling a larger range of structures from the MD simulation (for example, 3000 or 10000 structures) did not result in any new conformers. To test functional dependence, the lowest energy conformers were reoptimized with the M06 and B97-D approaches available with Gaussian 09 (revision A.02);[33] these did not reveal any significant changes to the trends obtained with the BP86 results.

Acknowledgment. We thank the EPSRC for financial support (L.J.L.H., M.J.P., S.E., M.A.N.) and Johnson Matthey plc for the kind loan of hydrated ruthenium trichloride.

Supporting Information Available: CIF files giving X-ray crystallographic data for $\mathbf{1a_{dppe}}$ and $\mathbf{1a_{^iPr/Ph}}$, experimental data for **7**, $\mathbf{3_{^iPr/Ph}}$, **10**, $\mathbf{3_{^iPr/H}}$, and $\mathbf{3_{Et/Me}}$, structural data for **7**, **10**, and $\mathbf{3_{Et/Me}}$, computed geometries and energies for all stationary points, and full refs 26 and 33. This material is available free of charge via the Internet at http://pubs.acs.org.

JA109702H

(30) (a) Ren, P.; Ponder, J. W. *J. Phys. Chem. B* **2003**, *107*, 5933. (b) Ren, P.; Ponder, J. W. *J. Comput. Chem.* **2002**, *23*, 1497. (c) Pappu, R. V.; Hart, R. K.; Ponder, J. W. *J. Phys. Chem. B* **1998**, *102*, 9725.
(31) Beeman, D. *J. Comput. Phys.* **1976**, *20*, 130.
(32) Berendsen, H. J. C.; Postma, J. P. M.; van Gunsteren, W. F.; DiNola, A.; Haak, J. R. *J. Chem. Phys.* **1984**, *81*, 3684.
(33) Frisch, M. J.; et al. *Gaussian 09*, revision A.02; Gaussian, Inc., Wallingford, CT, 2009.